Molybdenum LIF and NEXT Erosion Rate

IEPC-2015-221／ISTS-2015-b-221

Presented at Joint Conference of 30th International Symposium on Space Technology and Science
34th International Electric Propulsion Conference and 6th Nano-satellite Symposium, Hyogo-Kobe, Japan
July 4 – 10, 2015

Mark W. Crofton[1]
The Aerospace Corporation, El Segundo, CA, 90245, United States

Michael J. Patterson[2]
NASA Glenn Research Center, Cleveland, OH, 44135, United States

Abstract: Gridded ion engines sputter grid material into the plume, potentially reducing lifetime and generating deposits that alter spacecraft surface properties. Flux levels depend on angle with respect to the thrust axis, throttle conditions, grid material, and facility background pressure. The first LIF measurements of plume molybdenum for the NASA NEXT ion engine were performed and some of the initial results are presented. Dependence on facility background pressure, accelerator grid voltage, beam current and beam voltage has been studied, and the LIF signal was found to depend substantially on each of these parameters. The influence of pressure and accelerator grid voltage was slightly nonlinear under the conditions tested. The effect of beam current is thought to be linear to good approximation. Using approximate methods to normalize out the influence of accelerator grid voltage, background pressure, and beam current on erosion rate, the LIF signal at grid center was found to decrease significantly with increasing beam voltage. The magnitude of observed accelerator grid current is consistent with several-centimeter axial extent for collection of plume CEX ions. A number of results were readily explained, whereas others will require additional work.

[1] Senior Scientist, Propulsion Sciences Department, mark.w.crofton@aero.org
[2] Senior Technologist, Propulsion Division, michael.j.patterson@nasa.gov

I. Introduction

Gridded ion engines sputter grid material into the plume, potentially limiting thruster lifetime and producing deposits that alter spacecraft surface properties. Plume density and flux depend on angle with respect to the thrust axis, throttle level, grid material, and facility background pressure. Net mass deposition rates are also a function of ion beam flux, due to simultaneous removal of depositing species, and the ion beam flux varies strongly with angle. In contrast to the ion flux, molybdenum flux depends much more modestly on angle.

Ion engine grids are traditionally fabricated from molybdenum. This is the case for NSTAR, XIPS, and NEXT ion engines. An annular ion engine currently under development uses pyrolytic graphite (carbon) grids.[1] Other materials, especially titanium, have been considered in the past.[2] NASA's NEXT ion engine has a low grid sputter rate and long lifetime.[3] Since molybdenum plume density is approximately proportional to wear rate, for a given geometry, the low erosion rate of NEXT limits its molybdenum plume density and makes *in situ* detection more challenging. In spite of substantially higher grid lifetime compared to previous ion engine designs, the primary failure mechanism of the thruster is expected to result from degradation of the accelerator grid structure by ion sputtering effects. NEXT was designed with two extraction grids: screen and accelerator. Erosion occurs primarily on the accelerator grid, mainly from charge exchange ion impingement. Erosion rate can be studied by various techniques, including real-time imaging of grid apertures, post-test dimensional measurements, and real-time monitoring of erosion/deposition products. Limited prior work has been done on the latter. Fixed position and rotating quartz crystal microbalances (QCMs) were used previously to study plume deposition rates for NEXT[4] and the more erosive T5 ion engine.[5] The back-sputter of carbon from facility walls to thruster grids can potentially alter their erosion rate. Carbon back-sputter has been measured previously and its effect analyzed.[6,7]

QCM devices have been used successfully to measure differential sputter yield for molybdenum[8] and other metals, and carbon back-sputter rate from the test facility during NEXT lifetesting.[6] Real-time monitoring of plume molybdenum density via LIF or deposition via QCM can be challenging from a detection standpoint. The interpretation of QCM data is complicated by the low arrival rate and potential surface reactions with residual gas before the molybdenum is buried.

The first measurements of real-time accelerator grid erosion rate for the NEXT ion engine were obtained. The subset of laser-induced fluorescence (LIF) measurements described in this paper provide relative rather than absolute rate, and were targeted toward rate variation as a function of several selected operating parameters. The thruster was operated at numerous standard and extended throttle table conditions. Exploratory work was done on the effect of changing beam current and potentials on accelerator and screen grids. The effect of adding background xenon was also studied for a limited subset. The ion engine was operated at standard (TT10, developed for planetary science missions) and extended throttle table operating points,[9] but variation of accelerator (accel) grid voltage and background pressure was also performed around some operating points to study the effect. Two previous LIF studies of molybdenum in an ion engine plume have been performed.[10,11]

II. Experimental

A Coherent 899-21 ring dye laser pumped by a solid state Verdi V-8 laser at 532 nm was utilized for the measurements. The laser beam passed through the thruster plume approximately 1 cm downstream of grid center, transverse to the thrust axis. A photodiode near the far wall of the vacuum facility was used to verify or readjust the beam alignment. The dye laser fundamental passed through a frequency doubler, converting it to ultraviolet radiation, and up a periscope to a Brewster window port on the vacuum facility. Molybdenum atoms were excited from the ground state to an upper state that strongly fluoresces. The fluorescence was collected using a 15-cm diameter aluminum mirror and guided vertically upward through a window port to be focused into a 0.3 m McPherson 218 monochromator. The detector was a photomultiplier tube. The laser frequency was not scanned for the set of measurements included in this report. NEXT was operated in the Aerospace EP2 facility, which has 9.8m length and 2.4m diameter. Up to 10 CVI cryopumps of re-entrant and standard 1.2m designs can be operated simultaneously. The re-entrant pumps provide improved xenon pumping speed performance, with the drawbacks that chamber internal volume is lost and carbon backsputter rate is elevated. One set of LIF data was obtained for many different throttle levels, with the xenon background pressure in the Aerospace EP2 facility held constant at $\sim 7.7\times10^{-6}$ torr. When this was done, xenon gas was bled into the vacuum chamber through a sidewall port outlet about 1.8m from the thruster, at a plume angle of approximately 45 degrees, to control the background pressure. The principal pressure gage (Stabil-ion type ionization gage) for background measurements was 1.3m away, mounted off the chamber wall about 5 cm downstream from the grid apex. It did not have a line of sight view to the plasma inside the vacuum chamber. A second

Stabil-ion gage several meters downstream was found to read similar values when the gas bleed was active. For other measurements the background pressure was allowed to reach its natural level. During TL37 operation the xenon background established by the test facility with no gas bleed was 3.1×10^{-6} torr. A constant background of 7.8×10^{-6} torr across many throttle levels therefore is ~2.5× higher than the natural level associated with I_b = 3.52A, and this factor is higher for throttle points with lower beam current, I_b. By fixing the background pressure regardless of throttle condition it is eliminated as an experimental variable.

III. Results and Discussion

A. Facility Pressure Dependence

The pressure dependence of LIF signal and accelerator grid current (I_{acc}) measured for the throttle level (TL) 37 operating point (I_b = 3.52A, V_{acc} = -1180V), within the pressure range of 3.1×10^{-6} to 1.6×10^{-5} torr, is plotted in Fig. 1. Both exhibited strong variation with the background pressure. LIF signal extrapolates beautifully to near zero at zero background pressure, as shown in Fig. 2, suggesting that to a good approximation molybdenum plume production is solely a function of facility pressure for this operating point. On the other hand, the grid current extrapolates to about 10 mA, indicating that some current will be collected by the accelerator grid even under space conditions. The majority of ions collected by the grid at elevated pressure are known to be charge exchange ions, and these will impinge with energy directly relatable to the accel grid potential if they are formed at ~0V plasma potential (e.g. singly charged xenon ions strike the grid with about 200 eV kinetic energy if the grid potential is -200V). However, ions will impinge with a distribution of energies,[12,13] since the charge exchange and scattering interactions between beam ions and neutrals produce some energetic Xe^+ ions in addition to the slow ones. The energetic ions will be divergent with respect to the original direction of the Xe^+ ion before the charge exchange interaction. Neutrals can derive from either unionized source flow or background due to finite facility pumping speed. If the background pressure is zero, only source neutrals will be available for charge exchange/scattering interactions.

Ion impingement can avoid the production of significant levels of plume molybdenum if a) the ion energy impacting the grid is low (e.g. below 50 eV), b) the ion impact region is on the upstream face of the grid, or c) ion impacts occur only in a region of the grid aperture barrel with little or no view of the plume. If ions are moving upstream instead of downstream when they impact the barrel sputter efflux to the plume will be reduced but not eliminated; we do not include this in the above list. The situations listed are more likely to apply to the source flow contribution because – in contrast to the background gas – source neutral density is highest between the grids and decreases in the downstream direction. Charge exchange ions formed further downstream are considered to have enhanced probability of impinging on the downstream accel face.

We conclude that it is possible for charge exchange ions derived from the source flow and contributing to accel current to produce less increase of plume molybdenum density per unit of I_{acc}. On the other hand, we must expect to see some residual LIF signal when the facility pressure is zero. Therefore, even if background gas is substantially more effective at producing plume molybdenum than source gas, the data will make little sense if the source neutral density is higher than the background density throughout the region that matters. Source and background gas contributions obviously co-exist throughout the plume, and source gas density peaks near the grids where charge exchange interactions are greatest. Extrapolation of I_{acc} to zero pressure, as shown in Fig. 3, produces an intercept of about 10 mA. Inspection of Fig. 1 indicates that $\sim5\times10^{-6}$ torr background pressure doubles I_{acc}. We therefore take source and background I_{acc} contributions to be equal at this pressure. The expected I_{acc} contribution from background gas at 1.5×10^{-5} torr xenon pressure can be obtained from

$$I_{acc} = (5.3\times10^{11}cm^{-3})(5.5\times10^{-15}cm^{2})(3.52A)l_{cex} \tag{1}$$

where l_{cex} is the effective axial collection length for charge exchange ions by the accel grid. Since the observed value of I_{acc} is approximately 42 mA at the pressure of interest, with 10 mA of this ascribed to source neutrals the calculated value of l_{cex} is 31mm. This length is very similar to the value determined for the NSTAR ion engine.[14] Using the same collection length, we obtain 10 mA of accel current if the average source density is 1.6×10^{11} cm^{-3}, only slightly below the number we calculate. The substantial length of the collection volume makes the inter-grid contribution to I_{acc} (where source density is highest) a minor one. Still, molybdenum plume density associated with source gas production is anomalously low if the extrapolation shown in Fig. 2 is accurate. Part of the explanation probably lies with the source neutral density gradient and the relative ineffectiveness of upstream interactions compared to downstream. Since the above discussion does not fully explain an extrapolation to essentially zero LIF signal at null background pressure, we believe that the moly LIF trend will flatten out strongly if measured at lower pressure. The Aerospace Corporation facility was near the limit of its pumping speed capability for TL37 operation at ~3×10^{-6} torr background pressure, and therefore data were not obtained at lower pressure.

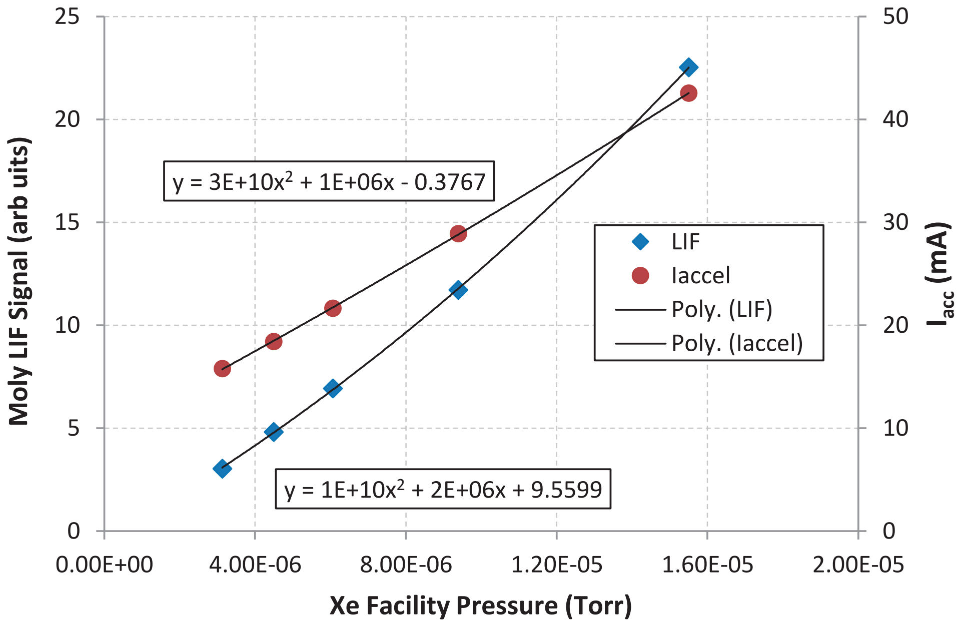

Figure 1. TL37 molybdenum LIF signal and accelerator grid current dependence on xenon background pressure in the test facility.

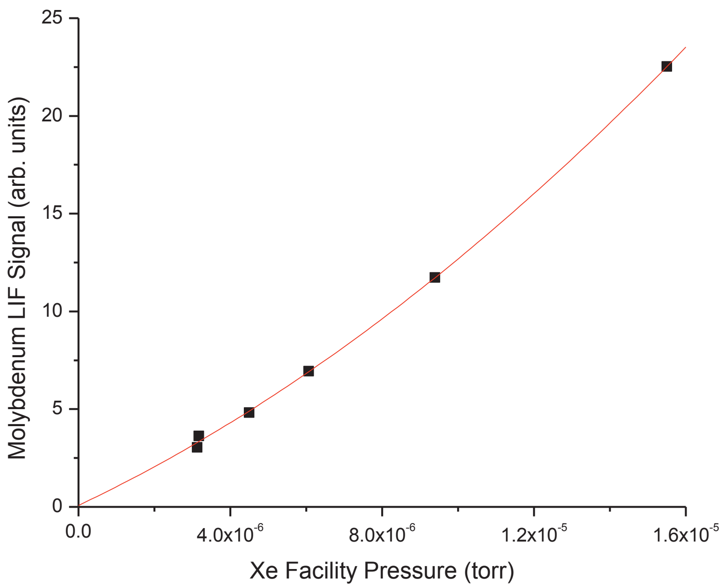

Figure 2. TL37 molybdenum LIF signal dependence on xenon background pressure in the test facility, showing extrapolated trend to space conditions (based on second order polynomial fit).

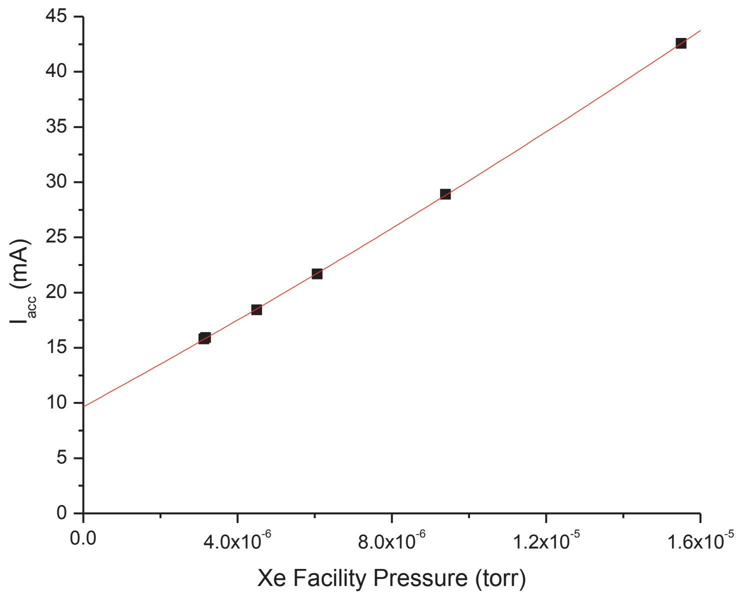

Figure 3. TL37 accelerator grid current extrapolation to space conditions, based on second order polynomial fit.

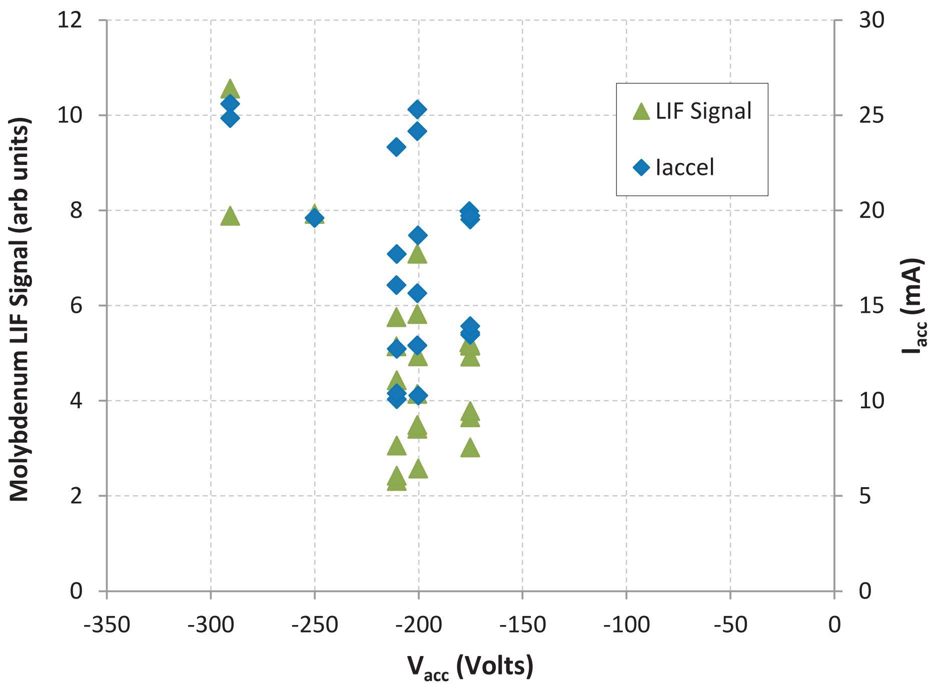

Figure 4. LIF signal and grid current plotted against accelerator grid voltage for selected throttle points with constant 7.7×10^{-6} torr facility background pressure.

B. Accelerator Grid Voltage Dependence

Observed LIF signal and I_{acc} values exhibit extensive scattering over a selected group of about 20 operating points as shown in Figure 4. While most of these operating points are nominally part of the standard NEXT throttle table, the facility background pressure was adjusted for each throttle level to maintain a constant value of about 7.7×10^{-6} torr. This was done to remove background pressure as a critical variable that affects LIF signal strength. A similar plot for the TL37 operating point only is given in Fig. 5, showing that regular trends exist for both LIF signal and accel impingement current when plotted against accel grid voltage (V_{acc}).

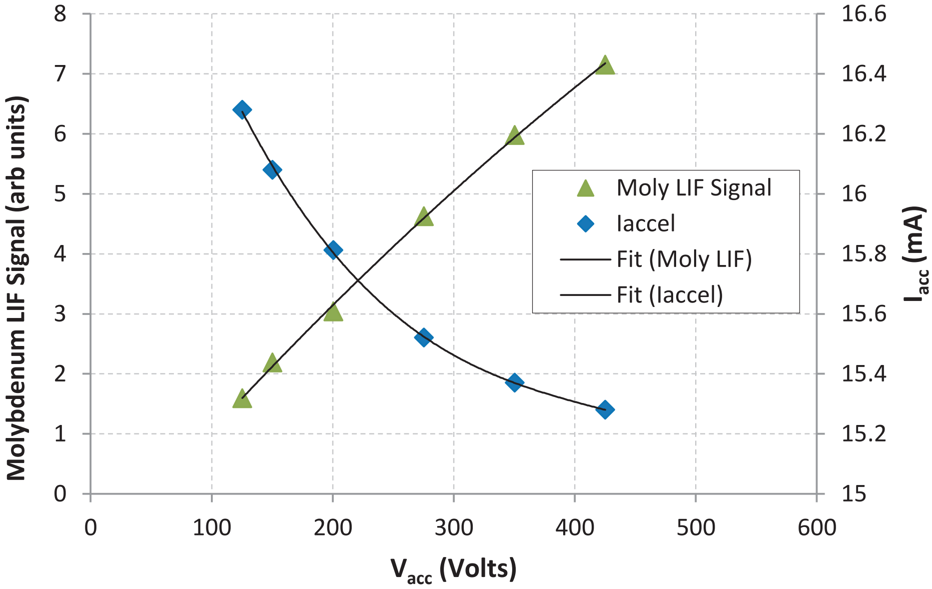

Figure 5. LIF signal and grid current dependence on accelerator voltage for TL37 throttle point.

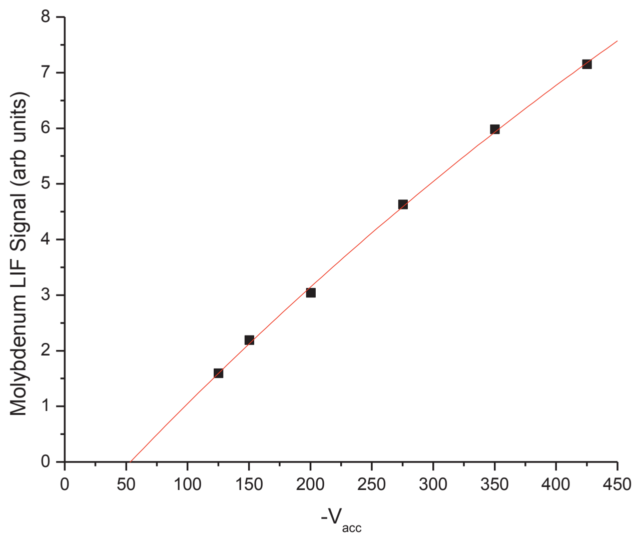

Figure 6. Extrapolated TL37 LIF signal dependence on accelerator grid voltage. Data were fit to the simple exponential function $y = y0 + A \exp(-V_{acc}/B)$.

The LIF signal fits well to an exponential function as shown in Fig. 6. Extrapolation to zero signal intersects V_{acc} at roughly -50V, approximately the "sputtering threshold" for molybdenum.[15] Exponential dependence of moly sputter yield at low energy has been established previously. The shape of the LIF signal vs V_{acc} is similar to measured normal incidence molybdenum sputter yield vs Xe^+ incident energy. The I_{acc} curve also follows an exponential trend, as shown by the fit in Figure 7. In percentage terms the I_{acc} variation is small, but it is still twice as large as the calculated dependence based on cross section measurements from guided ion beam results.[16] One candidate explanation for the decrease of I_{acc} with increasing total voltage (V_b – (-V_{acc})) is based on the increase of perveance and associated reduction of direct impingement current. However, the LIF signal does not appear to vary in the way expected if a direct impingement effect was significant.

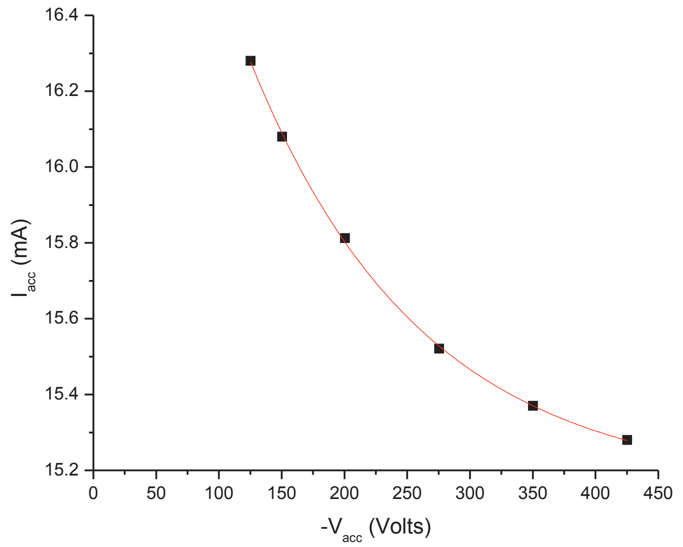

Figure 7. Accelerator grid current variation with grid voltage, fit to the exponential function $y = y0 + A$ exp(-V_{acc}/B).

C. Beam Voltage Dependence

The variation of accelerator grid current as beam current is varied, keeping other parameters constant, is plotted in Figure 8 for three beam voltage values. Each series is in the low to medium beam voltage category, and exhibits a linear relationship with beam current. Linearity is expected if the ion optics are performing well, since the accelerator grid current should depend on the product of I_b and some sort of neutral density function which is essentially constant. Because the background density is held constant and background dominates over source gas in producing accelerator grid impingement current, J_{acc} shows direct proportionality to I_b in the Figure. Each series extrapolates closely to zero grid current when beam current is nulled. The plot indicates that grid current is slightly reduced as beam voltage increases. In Fig. 9 the scale is expanded and additional throttle series for high beam voltage are added. Again, lower accelerator grid current is noticeable when the beam voltage is increased. However, the V_b=1800V data deviate from a straight line relationship, strongly departing from the established pattern at the highest current level. Close examination reveals that the deviations at 3.52A beam current form a consistent pattern for the entire set, as plotted in Fig. 10. The pattern follows an exponential function. Comparing the percentage difference for selected beam current values with different V_b to the calculated values based on known charge exchange cross sections, suggests that this variation may be due to the energy dependence of the cross sections.

We have already seen that LIF signal response to background pressure and V_{acc} is approximately linear in the regimes investigated. It is also reasonable to suppose that LIF signal is approximately proportional to the beam current. Therefore, we can normalize the signal to the product of V_{acc} and I_b. Since the background pressure was held as constant as possible for the 20 or so throttle points in question, pressure normalization is not necessary. The normalized signal is plotted in Fig. 11 vs beam voltage, revealing that plume molybdenum density falls off with increasing beam voltage. This runs contrary to the reasonable expectation that rising beam voltage will cause average kinetic energy of impinging ions to rise. One plausible explanation for plume molybdenum density reduction lies with screening effects; as the screen grid potential goes up, some charge exchange ions may be effectively blocked from backstreaming to the accelerator grid. An alternative explanation may be proposed based on perveance effects. The percentage change of LIF signal across the range of beam voltage is greater than the percentage change of I_{acc}, as would be expected, but the nearly linear LIF signal dependence on background pressure and beam current parameters argues against a perveance explanation. Effects of carbon backsputter from walls of the facility should also be considered.[6,7]

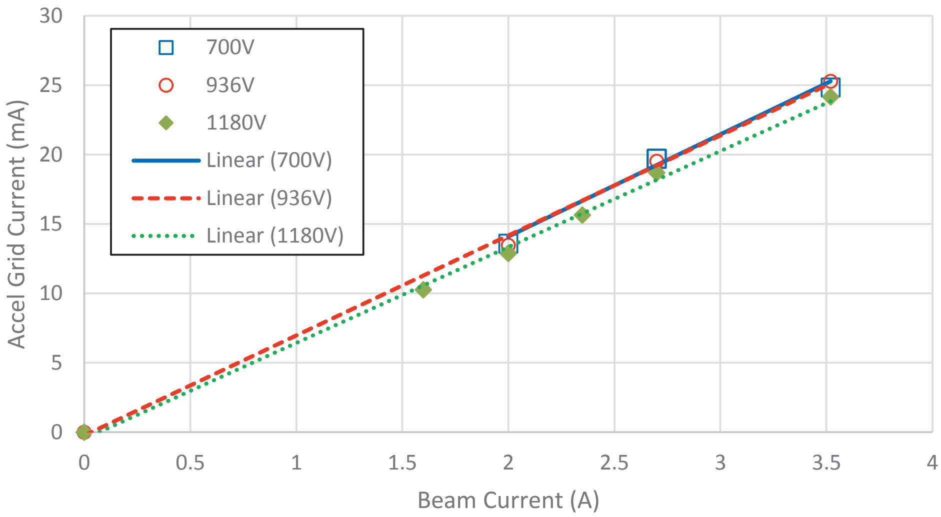

Figure 8. Accelerator grid current plotted as a function of beam current for three beam voltages with constant ion beam and grid voltages.

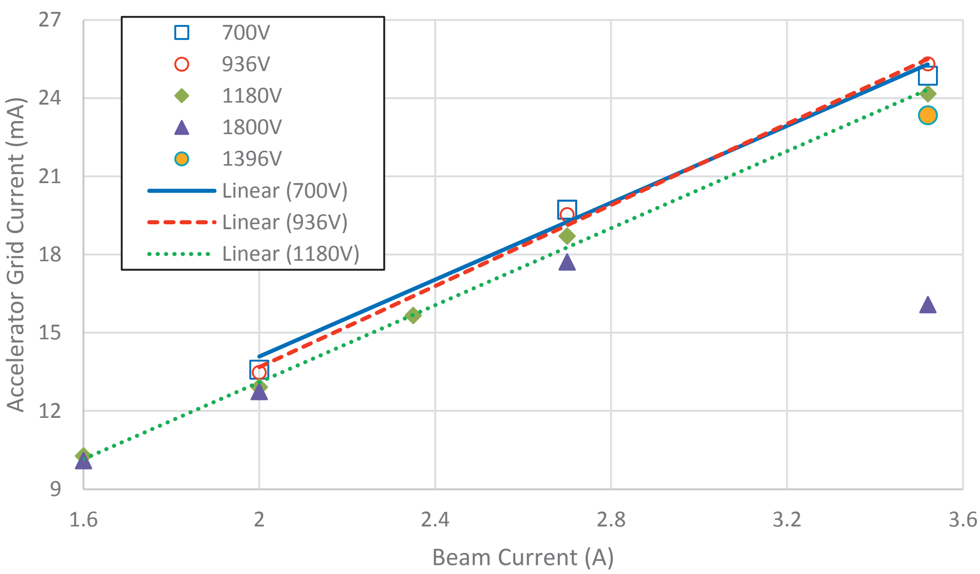

Figure 9. Accelerator grid current plotted for same three series shown in Fig 8, with expanded scale and two additional beam voltage settings.

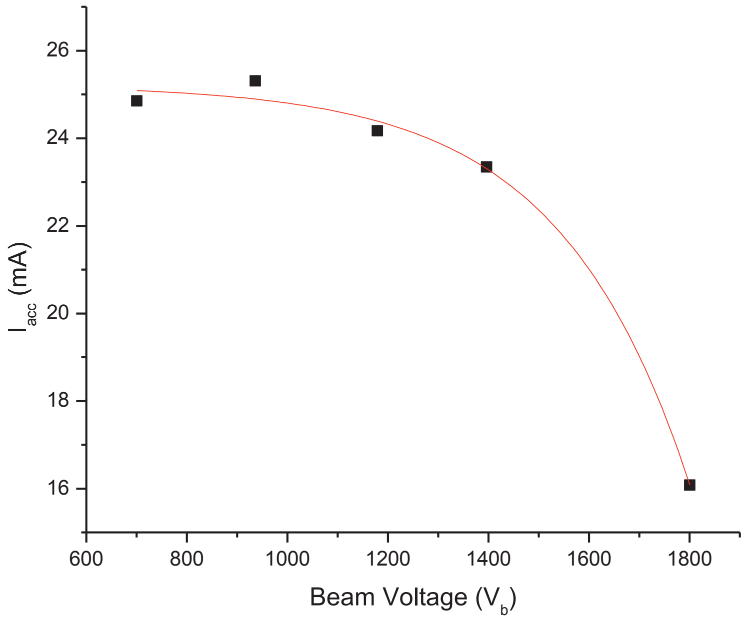

Figure 10. Accelerator grid current variation with beam voltage, under constant beam current conditions, fit to the exponential function $y = y0 + A \exp(-V_b/B)$.

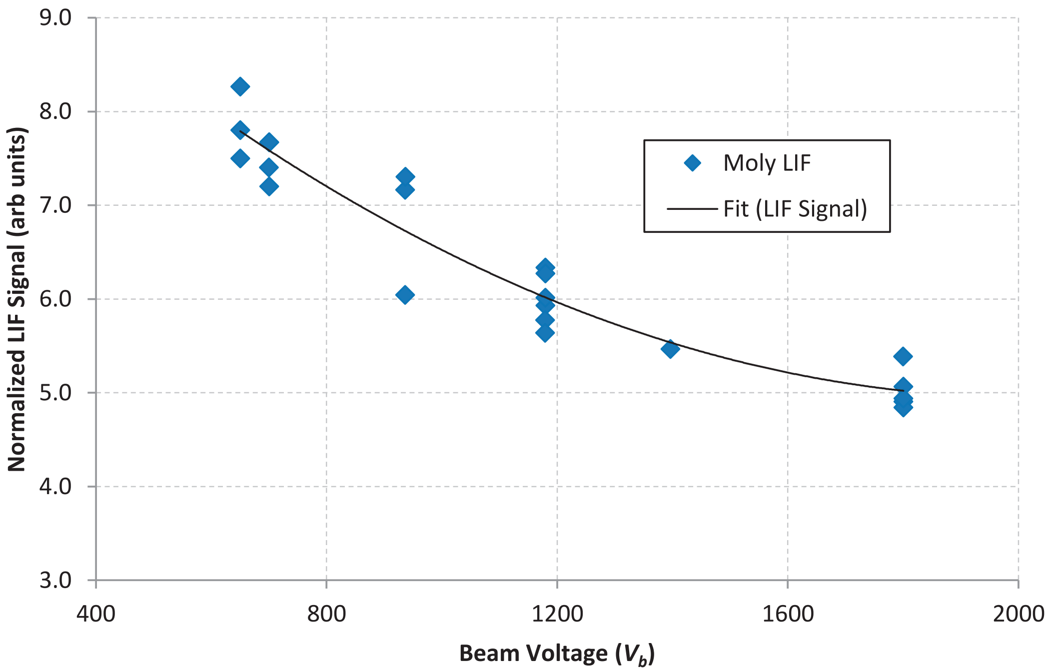

Figure 11. LIF signal variation, normalized by accelerator grid voltage and beam current, with beam voltage.

IV. Conclusion

A subset of the first molybdenum laser-induced fluorescence data to be collected in the plume of a NASA ion engine was presented and analyzed. Dependence on facility background pressure, accelerator grid voltage, beam current and beam voltage has been studied. The LIF signal was found to depend substantially on each of these parameters. The influence of pressure and accelerator grid voltage was slightly nonlinear under the conditions tested. The effect of beam current is thought to be linear to good approximation but the LIF signal was found to decrease significantly with increasing beam voltage. A number of results were readily explained, whereas others will require additional work.

V. Acknowledgments

This project was supported by NASA under Contract NNJ11HB94C to The Aerospace Corporation. The authors thank Kevin McCormick, Mike Worshum and Byron Zeigler for excellent technical support, and Jason Young for valuable assistance with data acquisition setup.

References

1. M.J. Patterson, J.E. Foster, J.A. Young, and M.W. Crofton, "Annular Engine Development Status," AIAA Paper 2013-3892, 49th Joint Propulsion Conference, San Jose, July 2013.
2. G.J. Williams, Jr., V.K. Rawlin, and G.C. Soulas, "Long Life, High Specific Impulse Titanium Ion Optics," AIAA Paper 2003-4866, Joint Propulsion Conference, Huntsville, 20-23 July 2003
3. R. Shastry, D. Herman, G.C. Soulas, and M.J. Patterson, "NASA's Evolutionary Xenon Thruster (NEXT) Long-Duration Test as of 736 kg of Propellant Throughput," AIAA Paper 2012-4023, 48th Joint Propulsion Conference, Atlanta, July-Aug 2012.
4. M.W. Crofton, J.C. Nocerino, J.A. Young, and M.J. Patterson, "NEXT Ion Engine Plume Deposition Rates: QCM Measurements," AIAA-2014-0140, SciTech, National Harbor, Maryland, January 2014.
5. L.N. Ahmed and M.W. Crofton, "Surface Modification Measurements in the T5 Ion Thruster Plume," *Journal of Propulsion and Power* **14** (1998), pp. 336-347.
6. C.-S. Ho, S. Banerjee, B.E. Koel, O.B. Duchemin, and J.E. Polk, "Desorption of Chemisorbed Carbon on Mo(100) by Noble Gas Ion Sputtering: Validation of Ground Test Measurements of Ion Engine Lifetimes," *Applied Surface Science* **252** (2006), pp 2657-2664.
7. G.C. Soulas, "The Impact of Back-Sputtered Carbon on the Accelerator Grid Wear Rates of the NEXT and NSTAR Ion Thrusters," IEPC-2013-157, 33rd International Electric Propulsion Conference, Washington DC, October 2013.
8. A.P. Yalin, J.D. Williams, V. Surla, J. Wolf, and K.A. Zoerb, "Azimuthal Differential Sputter Yields of Molybdenum by Low Energy Xe^+ Bombardment," AIAA Paper 2006-4336, 42nd Joint Propulsion Conference, Sacramento, July 2006.
9. M.J. Patterson, G.C. Soulas, J.A. Young, and M.W. Crofton, "Expanded Throttling Capabilities of the NEXT Thruster," AIAA Paper 2013-3891, 49th Joint Propulsion Conference, San Jose, July 2013.
10. C.J. Gaeta, J.N. Matossian, R.S. Turley, J.R. Beattie, J.D. Williams, and W.S. Williamson, "Erosion Rate Diagnostics in Ion Thrusters using Laser-Induced-Fluorescence," *J. Propulsion and Power* 9, 369 (1993).
11. M.W. Crofton, "Laser Spectroscopic Study of the T5 Ion Thruster," AIAA-95-2921, Joint Propulsion Conference, San Diego, July 1995.
12. I.D. Boyd and M.W. Crofton, "Grid Erosion Analysis of the T5 Ion Thruster," AIAA-2001-3781, 37th Joint Propulsion Conference, Salt Lake City, July 2001.
13. J.W. Emhoff and I.D. Boyd, "Grid Erosion Modeling of the NEXT Ion Thruster Optics," AIAA-2003-4868, 39th Joint Propulsion Conference, Huntsville, July 2003.
14. Goebel, Dan M., and Ira Katz. *Fundamentals of Electric Propulsion Ion and Hall Thrusters*. John Wiley and Sons Inc. Hoboken, NJ 2008, p. 229.
15. R.P. Doerner, D.G. Whyte, and D.M. Goebel, "Sputtering Yield Measurements during Low Energy Xenon Plasma Bombardment," *J. Applied Physics* 93 (9), 5816-23 (2003).
16. J.S. Miller, S.H. Pullins, D.J. Levandier, Y. Chiu, and R.A. Dressler, "Xenon Charge Exchange Cross Sections for Electrostatic Thruster Models," *J. Applied Physics* 91 (3), 984-991 (2002).